Trans. Phenom. Nano Micro Scales, 1(2):93-102, Summer – Autumn 2013
DOI: 10.7508/tpnms.2013.02.002

ORIGINAL RESEARCH PAPER

Moving Lids Direction Effects on MHD Mixed Convection in a Two-Sided Lid-Driven Enclosure Using Nanofluid

Javad Rahmannezhad[1], Mohammad Kalteh[2,*]
[1] *Department of Mechanical Engineering, University of Birjand, Iran*
[2] *Department of Mechanical Engineering, University of Guilan, Iran*

Abstract

Magnetohydrodynamic (MHD) mixed convection flow of Cu–water nanofluid inside a two-sided lid-driven square enclosure with adiabatic horizontal walls and differentially heated sidewalls has been investigated numerically. The effects of moving lids direction, variations of Richardson number, Hartmann number, and volume fraction of nanoparticles on flow and temperature fields have been studied. The obtained results show that for a constant Grashof number ($Gr = 10^4$), the rate of heat transfer increases with a decrease in the Richardson and Hartmann numbers. Furthermore, an increase of the volume fraction of nanoparticles may result in enhancement or deterioration of the heat transfer performance depending on the value of the Hartmann and Richardson numbers and the configuration of the moving lids. Also, it is found that in the presence of magnetic field, the nanoparticles have their maximum positive effect when the top lid moves rightward and the bottom one moves leftward.

Keywords: *Magnetic field; Mixed convection; Nanofluid; Numerical simulation; Two sided lid-driven*

1. Introduction

Mixed convection flow and heat transfer in enclosures is of great importance in many industrial heating or cooling applications namely solar collectors, float glass production and electronic devices. In this type of heat transfer, complicated patterns of heat and mass transfer occur because the flow driven by the movement of one or two faces creates a forced convection condition while temperature difference across the enclosure makes secondary buoyancy driven flow [1]. Besides, in applications where a great amount of heat needs to be ejected from a very small surface, the coolant should have more effective heat transfer characteristics. Heat transfer in such areas can be improved by using the nano fluids, owing to their high thermal conductivity and better stability. A comprehensive review of the nanofluid heat transfer characteristics can be found in [2] and [3]. Nanofluid natural convection heat transfer has been addressed in a large number of studies. Many authors like Khanafer et al. [4], Ece and Buyk [5], Aminossadati and Ghasemi [6], and Alloui et al.[7]investigated natural convection of nanofluids in enclosures. The results of studies about effects of nanofluids on mixed convection heat transfer in lid-driven cavities have been reported in the literature.

*Corresponding author
Email Address: mkalteh@guilan.ac.ir

Nomenclature		**Greek symbols**	
B_0	Magnetic field strength	α	thermal diffusivity
C_p	Specific heat, J/kg (K)	β	thermal expansion coefficient
g	gravitational acceleration (m/s^2)	ν	kinematic viscosity
L	enclosure height (m)	ξ	solid particle volume fractio
Ha	Hartmann number	μ	dynamic viscosity
k	Thermal conductivity (W/m K)	ρ	Density
Nu_{av}	average Nusselt number	σ	electrical conductivity
Nu_l	local Nusselt number on the left hot wall	ψ	stream function
Pr	Prandtl number	Ω	Vorticity
Ra	Rayleigh number	τ	nondimensioal time
Re	Reynolds number	θ	nondimensioal temperature
Ri	Richardson number	ω	nondimensioal vorticity
Gr	Grashof number	Ψ	nondimensioal stream function
T	dimensional temperature (K)		
u, v	dimensional velocity components (m/s)		**Subscripts**
U_0	lid velocity (m/s)	c	Cold
U, V	nondimensional velocity components	f	fluid phase
x, y	dimensional coordinates (m)	h	Hot
X, Y	nondimensional coordinates	nf	Nanofluid
		s	solid phase
		av	Average

Tiwari and Das [8] conducted a numerical study on the thermal behavior of Cu-water nanofluid in a two-sided lid-driven square enclosure with insulated horizontal walls and differentially heated sliding vertical walls. They found that the average Nusselt number increases with increase in the solid volume fraction. Another investigation was performed by Muthtamilselvan et al. [9], who have numerically examined the mixed convection in a lid-driven cavity filled with Cu-water nanofluid. Their numerical results showed that both the enclosure's aspect ratio and solid volume fraction affect the fluid flow and heat transfer of the enclosure. Nemati et al. [10] studied the mixed convection flows utilizing a water-based nanofluid containing Cu, Cuo or Al_2O_3 nanoparticles. They concluded that the effects of solid volume fraction grow stronger sequentially for Al_2O_3, Cuo and Cu. The effects of uncertainties of viscosity models for the Al_2O_3-water nanofluid on mixed convection in a square cavity was conducted by Arefmanesh and Mahmoodi [11]. Their results indicated that for both used viscosity models the average Nusselt number increases with increase in the volume fraction of the nanoparticles. Very recently, Abbasian Arani et al. [12] carried out a numerical simulation to investigate mixed convection flow of Cu-water nanofluid inside a lid-driven square cavity with sinusoidal heating on sidewalls. Effects of variations in Richardson number, phase deviation of sinusoidal heating, and volume fraction of nanoparticles on flow and temperature field were studied in their research. In many applied cases such as crystal growth, liquid metal casting blankets for fusion reactors, pumps, electronic packages and micro-electronic devices, the flow is influenced by magnetic fields. Hence, study on natural or mixed convection fluid flow and heat transfer in the enclosures in the presence of magnetic forces is important in such cases. There are a large number of studies on both MHD mixed and natural convection heat transfer in conventional fluid-filled enclosures. Groson et al. [13] have numerically studied the steady MHD free convection in a rectangular cavity filled with a fluid-saturated porous medium with internal heat generation. Rahman et al. [14] performed a numerical investigation into conjugate effect of joule heating and magnetic force, acting normal to the left vertical wall of an obstructed lid-driven cavity saturated with an electrically conducting fluid. Sivasankaran et al. [15] carried out a numerical study on mixed convection in a square cavity of sinusoidal boundary temperatures at the sidewalls in the presence of magnetic field. The results of a numerical study on mixed convection of MHD flow with joule effect in two-dimensional lid-driven cavity with corner heater were reported by Oztop et al. [16]. Revnic et al. [17] conducted a numerical investigation into the effects of an inclined magnetic field and heat generation on unsteady free convection within a square cavity filled with a fluid-saturated medium. The effects of moving lid direction on MHD-mixed convection in a cavity with linearly heated bottom wall were analyzed by Al-Salem et al. [1]. In spite of a large number of papers about natural and mixed convection of conventional fluids in cavities with magnetic field effects which is mentioned before, there is a serious lack of information about MHD natural or mixed convection of nanofluids in enclosures. Ghasemi et al. [18] examined the natural convection in an enclosure filled with water-Al_2O_3 nanofluid, influenced by a magnetic field. Natural convection in a square cavity filled with different nanofluids is studied numerically by Teamah et al. [19]. Both upper and lower surfaces were insulated, whilst a uniform magnetic field was applied in a horizontal direction. Nemati et al. [20] applied the Lattice Boltzmann method to investigate the effects of CuO nanoparticles on natural convection with MHD flow in a square cavity. To the best knowledge of the authors, the problem of mixed convection of a nanofluid in a two-sided lid-driven enclosure with magnetohydrodynamic effects has not been reported so far. Therefore, the aim and scope of the current study is to investigate the problem of mixed convection of a nanofluid in a two-sided lid-driven enclosure in the presence of a magnetic field. The influences of moving lids direction, variations of Richardson number, Hartmann number, and volume fraction of nanoparticles on flow and temperature field are studied. The results are presented in terms of streamlines, isotherms and average Nusselt number.

2. Problem definition and mathematical formulation

A two-dimensional square enclosure is considered for the present study with the physical dimensions shown in Fig. 1. In Fig. 1-a, the top wall of the enclosure moves rightward while its bottom wall moves leftward. This configuration will be referred to as RL. Similarly, other three configurations will be referred to as LR (Fig. 1-b), RR (Fig. 1-c) and LL (Fig. 1-d), respectively. In all configurations, the top and bottom walls are insulated whilst the left and right walls are kept at two different fixed temperatures. The enclosure is filled by a suspension of copper nanoparticles in water.

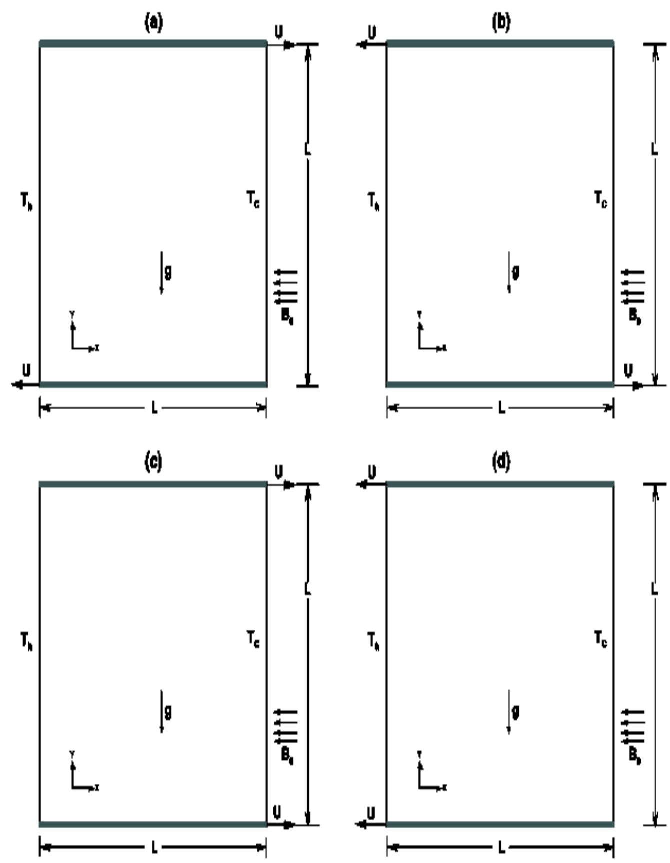

Fig. 1. Schematic flow configuration of the problem: a) RL Configuration, b) LR Configuration, c) RR Configuration and d) LL Configuration.

The shape and size of nanoparticles are supposed to be uniform. It is supposed that both the fluid phase and nanoparticles are in thermal equilibrium and there is no slip between them. The flow is supposed to be steady, laminar and two-dimensional. Thermophysical properties of water and copper at the reference temperature are presented in Table 1.

Table 1
Thermophysical properties of water and nanoparticles at 25^0 C.

Physical properties	Water	Cu
C_p(J/kg K)	4179	383
ρ(kg/m^3)	997.1	8954
k(W/m K)	0.613	400
$\beta\times10^{-5}$(K^{-1})	21	1.67

The properties of nanoparticles and fluid are assumed to be constant except for the density which varies according to Boussinesq approximation. Thus, the non-dimensional governing equations in a two-dimensional Cartesian coordinate system can be expressed as below:

$$\frac{\partial^2\psi}{\partial X^2}+\frac{\partial^2\psi}{\partial Y^2}=-\omega \tag{1}$$

$$\frac{\partial\omega}{\partial\tau}+U\frac{\partial\omega}{\partial Y}+V\frac{\partial\omega}{\partial Y}=\frac{1}{R_e}\frac{\nu_{nf}}{\nu_f}\left(\frac{\partial^2\omega}{\partial X^2}+\frac{\partial^2\omega}{\partial Y^2}\right)+R_i\frac{(\rho\beta)_{nf}}{\rho_{nf}\beta_f}\frac{\partial\theta}{\partial X}+\frac{Ha^2}{R_e}\frac{\partial V}{\partial X} \tag{2}$$

$$\frac{\partial\theta}{\partial\tau}+U\frac{\partial\theta}{\partial X}+V\frac{\partial\theta}{\partial Y}=\frac{K_{nf}}{K_f}\frac{(\rho c_p)_f}{(\rho c_p)_{nf}}+\frac{1}{RePr}\left(\frac{\partial^2\theta}{\partial X^2}+\frac{\partial^2\theta}{\partial Y^2}\right) \tag{3}$$

The following non-dimensional parameters are used to obtain the above equations:

$$X=\frac{x}{L},Y=\frac{y}{L},U=\frac{u}{U_0},V=\frac{v}{U_0}, \tag{4}$$

$$\tau=\frac{tU_0}{L},\omega=\frac{\Omega L}{U_0},\psi=\frac{\psi}{LU_0}$$

$$\theta=\frac{T-T_c}{T_h-T_c},Re=\frac{U_0L}{\nu_F},Pr=\frac{\nu_f}{\alpha_f}$$

$$Ri=\frac{Gr}{Re^2},\ Ha=B_0L\sqrt{\frac{\sigma_{nf}}{\rho_{nf}\nu_{nf}}}$$

where the density, thermal expansion coefficient, electrical conductivity, thermal diffusivity and heat capacity are as following, respectively:

$$\rho_{nf}=(1-\xi)\rho_f+\xi\rho_s \tag{5}$$

$$(\rho\beta)_{nf}=(1-\xi)(\rho\beta)_f+\xi(\rho\beta)_s \tag{6}$$

$$\sigma_{nf}=(1-\xi)\sigma_f+\xi\sigma_s \tag{7}$$

$$\alpha_{nf}=k_{nf}/(\rho c_p)_{nf} \tag{8}$$

$$(\rho c_p)_{nf}=(1-\xi)(\rho c_p)_f+\xi(\rho c_p)_s \tag{9}$$

The effective dynamic viscosity of the Cu–water nanofluid is calculated according to the Brinkman model [21] as follows:

$$\mu_{nf}=\mu_f(1-\xi)^{-2.5} \tag{10}$$

The effective thermal conductivity of the nanofluid is determined as follows [22]:

$$\frac{k_{nf}}{k_f}=1+\frac{k_s}{k_f}\frac{A_s}{A_f}+ck_sPe\frac{A_s}{k_fA_f} \tag{11}$$

Where k_s is the thermal conductivity of dispersed nanoparticles and k_f is the thermal conductivity of pure fluid. c is a constant and equal to 25000 for a wide range of experimental data [22], and:

$$\frac{A_s}{A_f}=\frac{d_f}{d_s}\frac{\xi}{1-\xi}\ ,\ Pe=\frac{u_sd_s}{\alpha_f} \tag{12}$$

where d_s is diameter of the solid nanoparticles that in this study is assumed to be equal to 100 nm, d_f is the molecular size of liquid that is taken as 2Å for water and also u_s is the Brownian motion velocity of nanoparticles given by:

$$u_s=\frac{2k_bT}{\pi\mu_fd_s^2} \tag{13}$$

where k_b is the Boltzmann constant.

The non-dimensional boundary conditions, used to solve the equations (1)-(3) are:

$$U = 0, V = 0 \text{ and } \theta = 1 \qquad \text{at left wall} \tag{14}$$

$$U = 0, V = 0 \text{ and } \theta = 0 \qquad \text{at right wall}$$

$$U = \pm 1, V = 0 \text{ and } \frac{\partial \theta}{\partial Y} = 0 \qquad \text{at bottom wall}$$

$$U = \pm 1, V = 0 \text{ and } \frac{\partial \theta}{\partial Y} = 0 \qquad \text{at top wall}$$

The local and average Nusselt numbers can present the local and average heat transfer rates of the enclosure. The local Nusselt number (Nu_l) is calculated along the left heated wall (Eq. (15)) and the average Nusselt number (Nu_{av}) is determined by integrating the local Nusselt number along the heated wall (Eq. (16)):

$$Nu_l = -\left(\frac{k_{nf}}{k_f}\right)\frac{\partial \theta}{\partial X} \tag{15}$$

$$Nu_{av} = \int_0^1 Nu_l dY \tag{16}$$

3. Numerical analysis and validation

The non-dimensional governing equations (Eqs. (1-3)) subjected to the boundary conditions (Eq. (14)) are solved by the finite difference scheme [23] and the system is numerically modeled in FORTRAN 95. The point Gauss–Seidel iterative method is used to solve the elliptic part of PDEs (Eq.1), and a fourth order Runge-Kutta method is employed to advance the solution of the parabolic parts (Eqs. 2-3).

To validate the numerical code, two different test cases are employed and the results are compared with the existing results. in the literature. The first test case is MHD mixed convection of air in a lid-driven square cavity with linearly heated bottom wall. The obtained results by the present code are compared with results of Al-Salem et al. [1] in Fig. 2.

The second test case is mixed convection of Al_2O_3–water nanofluid in a two-sided lid-driven cavity. The present results for the second test case are compared with results of Aminossadati et al. [24] in Table 2.

As shown in Fig. 2 and Table 2 there is a good agreement between the present results and the existing results in the literature.

The grid independence study is carried out by considering different mesh sizes for Ri=1, Ha=35 and ξ=0.06. Fig. 3 presents the average Nusselt number (Nu_{av}) for four different cases (RL), (LR), (RR) and (LL) which were introduced in Fig. 1. Based on the results, a grid size of 100×100 is found to meet the requirements of both the grid independency study and the computational time limits. The computations are performed until steady-state conditions are reached while a time-step equal to 10^{-3} sec is used. The convergence criterion used in the time loop to achieve steady-state condition is $\left|\varphi^k - \varphi^{k-1}\right| < 10^{-6}$, where φ stands for either θ or ω.

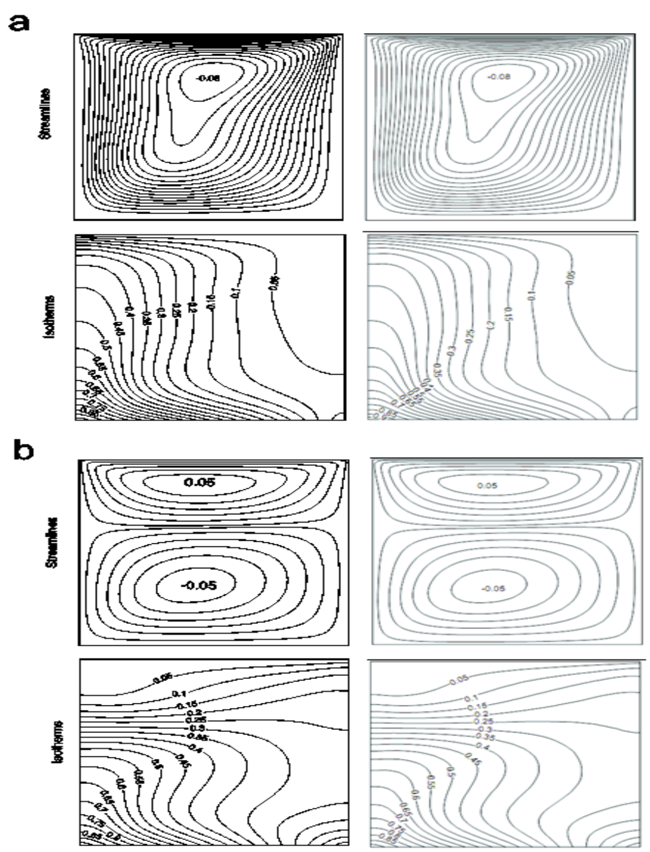

Fig. 2. Comparison between present results (right column) and results of Al-Salem et al. [1] (left column) for two cases: a)The lid is moving in +X direction and b) The lid is moving in –X direction, (Re=100, Gr=10^5, Ha=30).

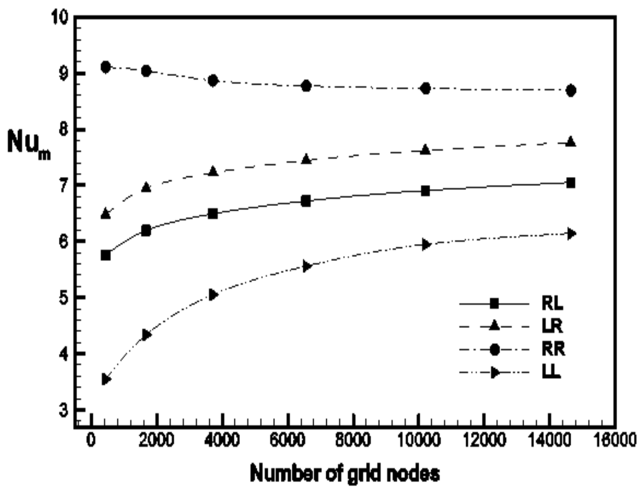

Fig. 3. Grid independency study: average Nusselt number at different grid densities.

5. Results and discussion

In this section, results of the numerical study of mixed convection flow and heat transfer inside the two-sided lid-driven square enclosure using Cu-water nanofluid that was shown in Fig. 1 are presented. The results have been obtained for Richardson number ranging from 0.1 to 10, the Hartmann number ranging from 0 to 55, and the volume fraction of the nanoparticles ranging from 0 to 0.06. It must be noted that in the present study, the Richardson number is varying with variation of Reynolds number while Grashof number is kept constant at 10^4.

Fig. 4 shows streamlines and isotherms for four different configurations at Ri=1 and Ha=35. The results are presented for pure fluid (dashed line) and nanofluid with ξ=0.06 (solid line). As can be seen from this figure, in all cases two large fully developed eddies are formed inside the enclosure due to shear forces exerted on the nanofluid next to the walls. In the case (a) where the top moving lid moves rightward and the bottom one moves leftward, the effects of moving leads amplifies buoyancy force and opposes the effect of magnetic force. Due to the motion of the two walls, two major clockwise recirculation cells are produced inside the enclosure. The direction of this rotation is according to the direction of shear forces exerted by moving leads. It is worth mentioning that nanoparticles have a considerable effect on the flow pattern so that their addition intensifies the strength of vortexes.

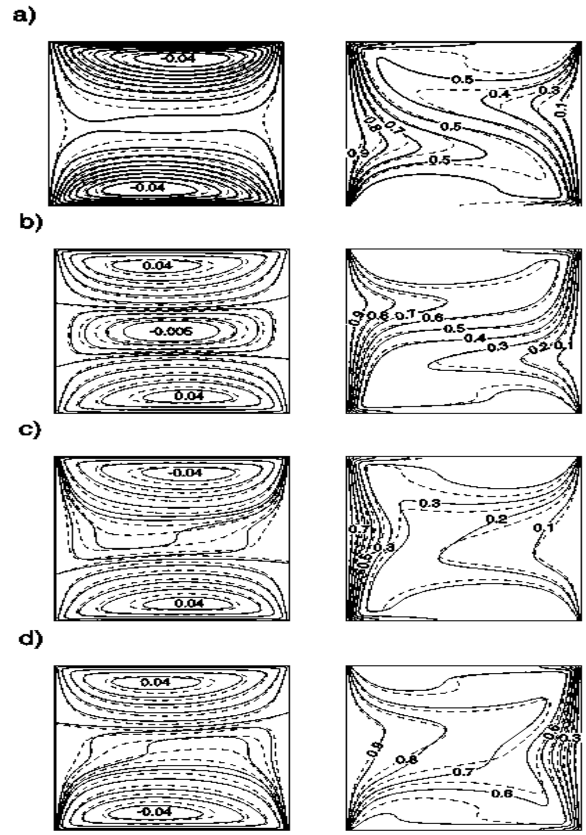

Fig. 4. Streamlines (on the left) and isotherms (on the right) for Cu-water nanofluid with ξ=0.06 (solid line) and pure fluid (dashed line) a) RL, b) LR, c) RR and d) LL configuration (Ri=1, Ha=35).

The isotherms in the left column of Fig.4a shows that the heat transfer has a good balance and the heat is well distributed in the whole regions of the enclosure. It is obvious from this figure that the temperature gradient is high in the vicinity of the right wall which means high rate of heat transfer in this region. In the case (b), each wall moves in the opposite direction of corresponding wall of the case (a). Similar to the previous case, the streamlines near the moving walls include two major recirculation cells, but the direction of rotation is counterclockwise in this case. Moreover, there is a weaker clockwise circulating zone in the middle of the enclosure which is generated due to the dominance of magnetic forces in this region. Fig. 4c is related to the third studied configuration named as RR. In this configuration, both top and bottom walls move rightward and hence the generated vortexes are in opposite direction. Due to the conformity of the top wall force, buoyancy force and magnetic force in the middle region, the top recirculation cell penetrated deeper in the enclosure.

Table 2

Comparison of average Nusselt numbers from the present code against S.M. Aminossadati et al. [22].

		Solid volume fraction		
		0	**0.02**	**0.04**
Same direction	Present study	6.133	6.341	6.549
	S.M. Aminossadati et al. [24].	5.802	6.099	6.392
	Difference	5.40%	3.97%	2.46%
Opposite direction	Present study	5.402	6.178	7.159
	S.M. Aminossadati et al. [24].	5.206	6.036	7.041
	Difference	3.76%	2.35%	1.68%

The isotherms demonstrate that the temperature gradients are higher near the hot wall. This implies higher heat transfer rate in this region. In the last configuration (Fig. 4d), both top and bottom walls move leftward and hence again the two major generated vortexes are in opposite direction and also against the vortexes in the RR configuration. Here, the magnetic force augments the bottom wall shear force and hence the underneath recirculation cell penetrates deeper in the enclosure.

Variations of average Nusselt number with Richardson number at four different configurations are shown in Fig. 5.

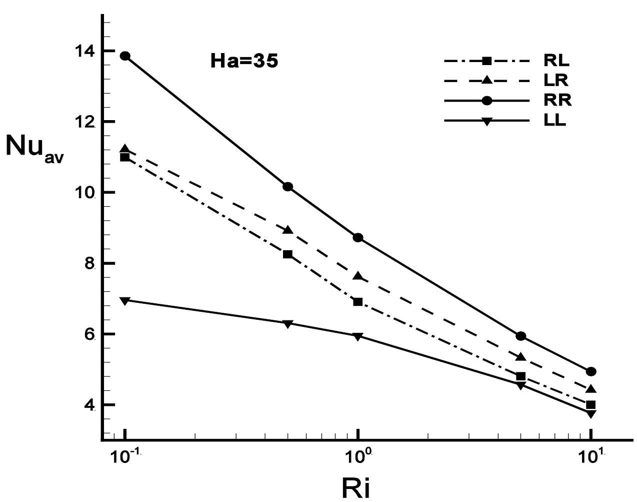

Fig. 5. Variations of average Nusselt number with Richardson number at four different configurations (ξ=0.06).

According to the figure, as Richardson number increases, while the Grashof number is kept constant, the effect of top and bottom walls and forced convection decreases. So the average Nusselt number decreases as a result of weaker convective flows.

Moreover, it can be seen that the maximum and minimum average Nusselt numbers are related to RR and LL configurations, respectively. This is quiet consistent because in the RR configuration the forces generated by the two walls are in the same direction and they oppose the magnetic force, while, in the case of LL configuration, the effects of two moving lids and the magnetic force are all in the same direction. The Nusselt numbers of RL and LR configurations are lower than that of RR configuration. The reason is that in the RL and LR cases, the walls move in such a way that their resultant forces are in the opposite directions.

In order to expose the magnetic field effects on the heat transfer rate, variation of the average Nusselt number with the Hartmann number has been tracked. Fig. 6 shows how this number varies with respect to the direction of moving lids at different values of the Hartmann number.

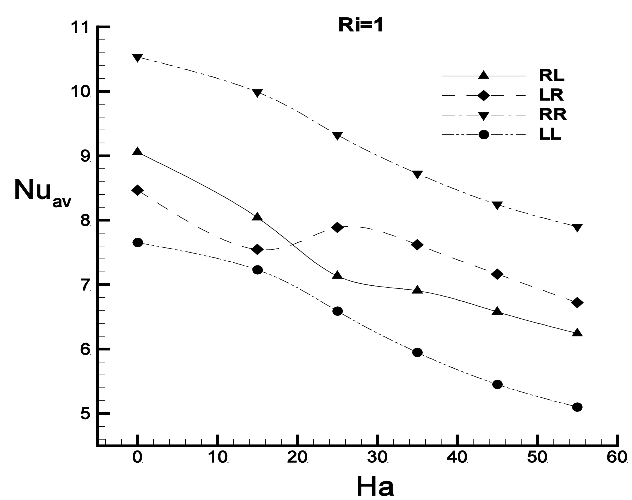

Fig. 6. Variations of average Nusselt number with Hartmann number at four different configurations (ξ=0.06).

The results indicate that except for the small region of the LR configuration, the heat transfer rate decreases with an increase in magnetic field strength. This behavior can be described according to the combined effects of moving lid forces and the magnetic force on each configuration. Again it is obvious that the maximum and minimum Nusselt numbers is related to RR and LL configurations, respectively.

Fig. 7 shows the variation in the average Nusselt number ratio ($\mathrm{Nu}_{av} / \mathrm{Nu}_{av,\xi=0}$) against the solid particle volume fractions for different configurations at different values of the Richardson number. The average Nusselt number ratio at ξ=0 is the reference value and the Hartmann number is assumed to be constant (Ha=35) for this part of the study. As can be seen from this figure, at low Richardson numbers, the maximum positive effect of nanoparticles is related to the RL configuration. It is notable that in some cases, the addition of nanoparticles deteriorates the heat transfer performance in the enclosure especially in higher Richardson numbers in which natural heat transfer is dominant. Variations of the average Nusselt number ratio with the solid particle volume fractions at different Hartmann numbers and for four different configurations are depicted in Fig. 8. As illustrated in this figure, the effect of nanoparticles is more pronounced for lower values of the Hartmann number. For example in the RL configuration at ξ=0.06 when the Hartmann number varies from 0 to 55, the improvement in the average Nusselt number due to addition of nanoparticles decreases from 5.5% to 1.7%.

4. Conclusion

In the present work the problem of MHD mixed convection flow of Cu–water nanofluid inside a two-sided lid-driven square enclosure with adiabatic horizontal walls and differentially heated sidewalls were numerically studied. The governing equations were solved using finite difference scheme. According to the obtained results, it can be concluded that

-Depending on the value of Hartmann and Richardson numbers and the configuration of the moving lids, both enhanced and deteriorated heat transfer were observed by addition of nanoparticles.

-For a constant Grashof number, when the Richardson and Hartmann numbers decrease, the rate of heat transfer increases.

-In the existence of magnetic field, the nanoparticles have their maximum positive influenceon the heat transfer rate in the RL configuration.

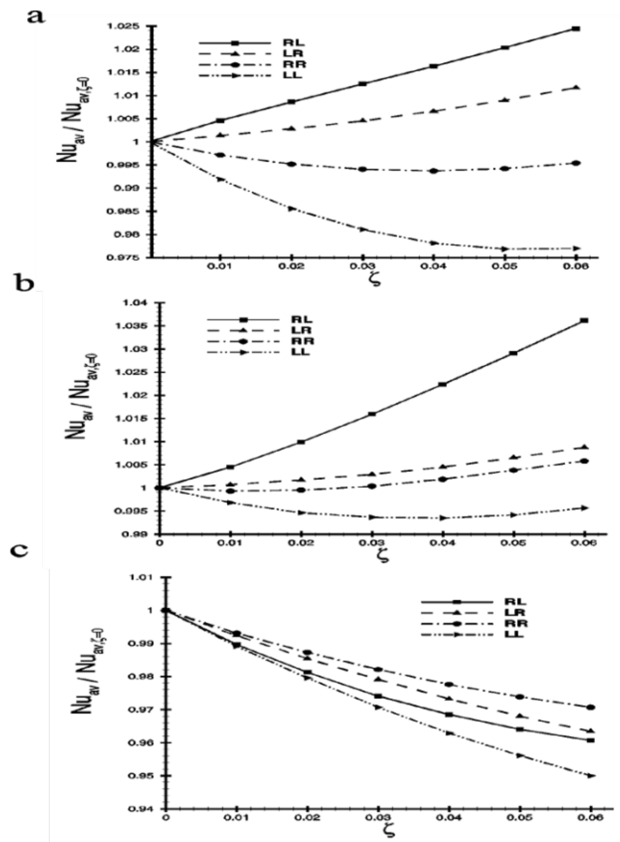

Fig. 7. Variations of the average Nusselt number ratio at hot wall with solid volume fraction at Ha=35 for different configurations a) Ri=0.1, b) Ri=1, c) Ri=10.

.

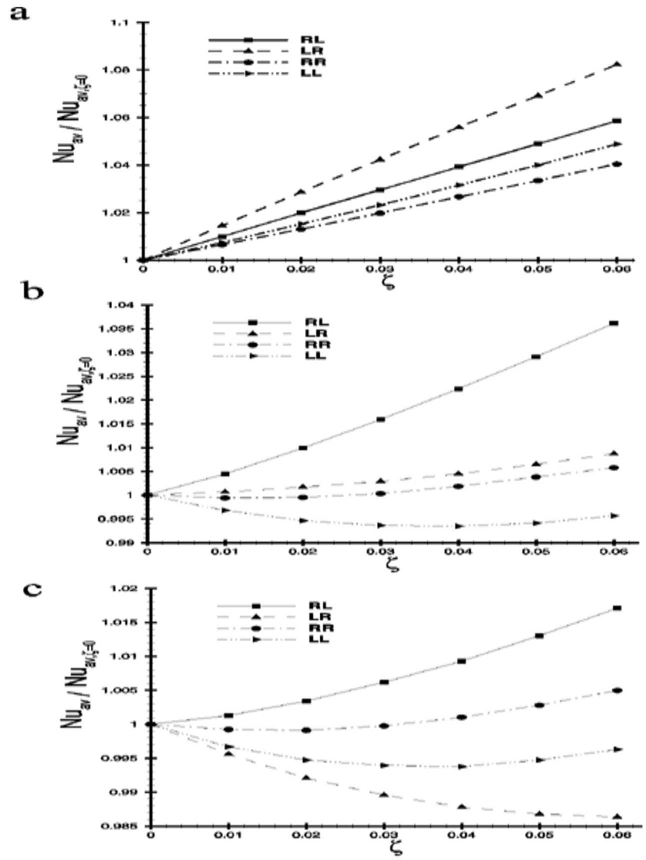

Fig. 8. Variations of the average Nusselt number ratio at hot wall with solid volume fraction at Ri=1 for different configurations a) Ha=0, b) Ha=35, c) Ha=55.

References

[1] Kh. Al.Salem, H. F.Öztop, I. Pop, Y.Varol, Effects of moving lid direction on MHD mixed convection in a linearly heated cavity, Int. J. Heat Mass Transf. 55 (2012) 1103-1112.

[2] J. Sarkar, A critical review on convective heat transfer correlations of nanofluids, Renewable and Sustainable Energy Reviews. 15 (2011) 3271-3277.

[3] L. Godson, B. Raja, D.M. Lal, S. Wongwises, Enhancement of heat transfer using nanofluids-An overview, Renewable and Sustainable Energy Reviews. 14 (2010) 629-641.

[4] K. Khanafer, K. Vafai, M. Lightstone, Bouyancy-driven heat transfer enhancement in a two-dimensional enclosure utilizing nanofluid, Int. J. Heat Mass Transf. 46 (2003) 3639-3653.

[5] M.C. Ece, E. Buyuk, Natural-convection flow under a magnetic field in an inclined rectangular enclosure heated and cooled on adjacent walls, Fluid Dynamics Research 38 (8) (2006) 564-590.

[6] S.M. Aminossadati, B. Ghasemi, Natural convection cooling of a localized heat source at the bottom of a nanofluid-filled enclosure, European Journal of Mechanics- B/Fluids 28 (2009) 630-640.

[7] Z. Alloui, P. Vasseur, M. Reggio, Natural convection of nanofluids in a shallow cavity heated from below, International journal of Thermal sciences 50 (2011) 385-393.

[8] R.K. Tiwari, M.K. Das, Heat transfer augmentation in a two-sided lid-driven differentially heated square cavity utilizing nanofluids, International Journal of Heat and Mass Transfer 50 (2007) 2002-2018.

[9] M. Muthtamilselvan, P. Kandaswamy, J. Lee, Heat transfer enhancement of copper-water nanofluid in a lid-driven enclosure, Communications in Nonlinear Science and Numerical Simulations 15 (2010) 1501-1510.

[10] H. Nemati, M. Farhadi, K. Sedighi, E. Fattahi A.A.R Darzi, Lattice Boltzmann simulation of nanofluid in lid driven cavity, International Communications of Heat and Mass Transfer 37 (2010) 1528-1534.

[11] A. Arefmanesh, M. Mahmoodi, Effects of uncertainties of viscosity models for Al_2O_3-water nanofluid on mixed convection numerical simulations, International journal of Thermal sciences 50 (2011) 1706-1719.

[12] A.A. Abbasian Arani, S. Mazrouei Sebdani, M. Mahmoodi, A. Ardeshiri, M. Aliakbari, Numerical study of mixed convection flow in a lid-driven cavity with sinusoidal heating on sidewalls using nanofluids, Superlattices and Microstructures 51 (2012) 893-911.

[13] T. Grosan, C. Revnic, I. Pop, D.B. Ingham, Magnetic field and internal heat generation effects on the free convection in a rectangular cavity filled with a porous medium, International Journal of Heat and Mass Transfer 52 (2009) 1525–1533.

[14] M.M. Rahman, M.A. Alim, M.M.A. Sarker, Numerical study on the conjugate effect of joule heating and magneto-hydrodynamics mixed convection in an obstructed lid-driven square cavity, International Journal of Heat and Mass Transfer 37 (2010) 524–534.

[15] S. Sivasankaran, A. Malleswaran, J. Lee, P. Sundar, Hydro-magnetic combined convection in a lid-driven cavity with sinusoidal boundary conditions on

both sidewalls, International Journal of Heat and Mass Transfer 54 (2011) 512–525.

[16]H. F. Oztop, Kh. Al-Salem, I. Pop, MHD mixed convection in a lid-driven cavity with corner heater, International Journal of Heat and Mass Transfer 54 (2011) 3494–3504.

[17] C. Revnic, T. Grosan, I. Pop, D.B. Ingham, Magnetic field effect on the unsteady free convection flow in a square cavity filled with a porous medium with a constant heat generation, International Journal of Heat and Mass Transfer 54 (2011) 1734–1742.

[18] B. Ghasemi, S.M. Aminossadati, A. Raisi, Magnetic field effect on natural convection in a nanofluid-filled square enclosure, International Journal of Thermal Sciences. 50 (2011) 1748-1756.

[19]M.A.Teamah,W.M.El-Maghlany, Augmentation of natural convective heat transfer in square cavity by utilizing nanofluids in the presence of magnetic field and uniform heat generation/absorption, International Journal of Thermal Sciences 58 (2012) 130-142.

[20] H. Nemati, M. Farhadi, K. Sedighi, H.R. Ashorynejad, E. Fattahi, Magnetic field effects on natural convection flow of nanofluid in a rectangular cavity using the Lattice Boltzmann model, Scientia Iranica B 19 (2012) 303–310.

[21]H.C. Brinkman, The viscosity of concentrated suspensions and solutions, Journal of Chemical Physics 20 (1952) 571–581.

[22]H.E. Patel, T. Pradeep, T. Sundararajan, A. Dasgupta, N. Dasgupta, S.K. Das, A micro- convection model for thermal conductivity of nanofluid, Pramana-J. Phys. 65 (2005) 863–869

[23]K.A.Hoffmann, S.T. Chiang, Computational Fluid Dynamics,Engineering Education System. 1 (2000).

[24] S.M. Aminossadati, A. Kargar, B. Ghasemi, Adaptive network-based fuzzy inference system analysis of mixed convection in a two-sided lid-driven cavity filled with a nanofluid, International Journal of Thermal Sciences. 52 (2012) 102-111.